The Radiofrequency Spectra of the Sodium Halides

W. A. NIERENBERG AND N. F. RAMSEY
Columbia University, New York, New York

(Received August 11, 1947)

The radiofrequency spectra of $Na^{23}Br$, $Na^{23}Cl$, and $Na^{23}I$ have been investigated by use of the molecular-beam resonance method. In external fields of approximately 10,000 gausses, the spectra are about 1 Mc/sec. wide, continuous, and of a characteristic form with a deep central minimum and two smaller side minima. The central minimum agrees in frequency to 0.2 percent with the Larmor frequency for a decoupled Na^{23} nucleus. At this field the orientation-dependent interaction of the Na^{23} nucleus with the molecule is small compared to the interaction of the nuclear magnetic moment with the external magnetic field. Comparison of the observed spectra with the statistical theory of Feld and Lamb suggests that the effect is due to the interaction of an electric quadrupole moment of the sodium nucleus with the inhomogeneous electric field of the other charges in the molecule. In this theory, the continuous nature of the spectrum is a result of the large number, $2J+1$, of magnetic states of the molecule for large rotational quantum numbers, J. The triple minima are characteristic of nuclear spin $\frac{3}{2}$. The spectra were further studied in progressively lower fields. The marked loss of character of the spectra for intermediate fields is explained by extending the analysis of the $\cos^2(\mathbf{I}, \mathbf{J})$ coupling. In the limit of zero field (resonance minima of a type not heretofore observed) a single resonance is observed for each compound at a frequency equal to the frequency difference between the side minima observed in strong fields for the same compound. This is in good agreement with the predictions of Feld and Lamb. These frequencies are 1.22, 1.42, and 0.99 Mc/sec. for NaBr, NaCl, and NaI, respectively. The theory of the behavior of the central minimum as a function of the external field, and the effect of the finite resolution of the apparatus are developed more fully, particularly insofar as they affect the ultimate precision of measurements of nuclear g-factors and nuclear quadrupole interactions. The analysis of the spectra indicates the possibility of still an additional interaction of the form $c\mathbf{I}\cdot\mathbf{J}$, whose average value is 0.05 Mc/sec. This is about 25 times larger than the interaction which would be caused by the magnetic field of a charge of one electron rotating at the internuclear distance of the molecule and with its average angular velocity. This possibility is supported by the need for introducing a term of this nature in the Hamiltonian for LiF in order to explain the observed width of 0.5 Mc/sec. for the F resonance.

I. INTRODUCTION

THE molecular-beam radiofrequency resonance method[1–3] has been extensively used to measure the magnetic moments of a large number of nuclei with precisions ranging from 0.5 to 0.02 percent. With this method, the absorption and stimulated emission spectrum of a molecule in a homogeneous magnetic field is obtained by observing the reduction in beam intensity resulting from the failure of magnetic refocusing for molecules which have made a transition accompanied by a change in the effective component of magnetic moment along the field direction. Analysis of the discrete minima observed in the radiofrequency spectrum of HD and D_2[2,4] has yielded the quadrupole moment of the deuteron and the rotational magnetic moment of the hydrogen molecule. Broadening of the minima of other spectra has been reported by Millman and Kusch[5] for cases of rotational $J \gg 1$, but further investigation was limited by the lack of a statistical theory at the time.

A preliminary report of the investigations of the spectrum of Na^{23} in NaBr, NaCl, and NaI has already been published.[6] This paper gives a

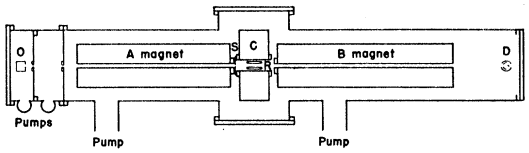

FIG. 1. Block diagram of the molecular-beam apparatus. The A and B magnets supply the inhomogeneous focusing fields, C indicates the homogeneous field, and R the oscillating field. The first chamber on the left, O, is the oven or source chamber, the slit marked S is the collimator, and D indicates the position of the hot-wire detector.

[1] Rabi, Millman, Kusch, and Zacharias, Phys. Rev. **55**, 526 (1939).
[2] Kellogg, Rabi, Ramsey, Jr., and Zacharias, Phys. Rev. **56**, 728 (1939).
[3] J. M. B. Kellogg and S. Millman, Rev. Mod. Phys. **18**, 323 (1946).
[4] Kellogg, Rabi, Ramsey, and Zacharias, Phys. Rev. **57**, 677 (1940).
[5] P. Kusch, S. Millman, and I. I. Rabi, Phys. Rev. **55**, 1176 (1939).
[6] W. A. Nierenberg, N. F. Ramsey, and S. B. Brody, Phys. Rev. **70**, 773 (1946).

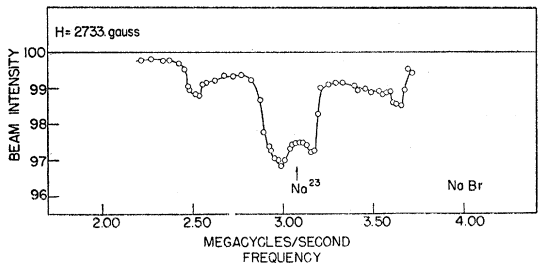

FIG. 2. Radiofrequency spectrum of NaBr. The radiofrequency current is 10 amperes. The arrow indicates the position at which the resonance of the Na^{23} nucleus would appear if there were no orientation—dependent interaction. Note that even at this low field the two side minima and the deeper central minimum are in evidence. At this field the interaction of the Na^{23} nucleus with the external field is larger than the orientation-dependent interaction of the nucleus with the molecule.

more complete account of the work on the spectra. Particularly, the experimental and theoretical arguments justifying the assumption of a sufficiently large electrical quadrupole interaction to cause the observed spectrum are developed.

II. APPARATUS AND METHOD

The apparatus is basically one built in 1938 by Millman and Kusch.[1] Figure 1 is a block diagram of the apparatus. The important dimensions are the lengths of the A and B inhomogeneous magnetic fields, 53 cm and 59 cm, respectively, and the C homogeneous field, 10 cm. The distance from the oven slit to the collimator slit is 68 cm and from the collimator to the detector is 96 cm. The oven slit is 0.025 mm wide, the collimator 0.035 mm wide, and the detector is a tungsten wire 0.025 mm in diameter. The "throwout" power of the apparatus for the sodium halides is 60 percent. It is measured by observing the decrease in beam intensity caused by the deflecting A field when the refocusing B field is zero. The oscillating magnetic field is 10 cm long. A typical oven operating temperature is 1000°K, and for this temperature the average velocity of a molecule of NaCl in the beam is 50,000 cm/sec. This corresponds to a resolution (half-width of a line) of 5000 cycles/sec. The homogeneous field was calibrated to 0.2 percent, using the resonance of Li^7 in LiBr and LiF^7.

The regions in which spectra are observed are approximately 10^6 sec.$^{-1}$ wide. Assuming these spectra arise from broadening of the nuclear resonance in the external field caused by internal interactions, then even at the strongest fields available (corresponding to a Na^{23} nuclear resonant frequency of 10^7 sec.$^{-1}$) the internal interaction is about 10 percent of the magnetic interaction and hence varying the magnetic field would change the coupling by several percent. Therefore, all runs in this research were made with a fixed magnetic field and variable oscillator frequency. The observations were made by switching the oscillator on and off and observing the resultant change in beam intensity.

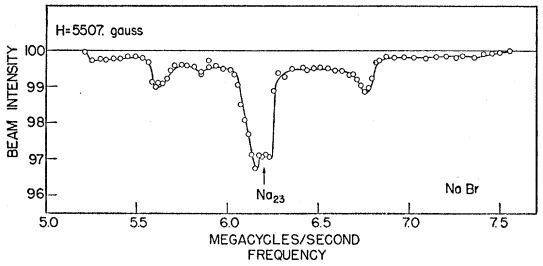

FIG. 3. Radiofrequency spectrum of NaBr at approximately double the field of Fig. 2 and 8-amperes radiofrequency current. The minima are more clearly in evidence. The central minimum in particular is deeper and narrower. Note the appearance of the plateaus on either side of the side minima (compare Fig. 14).

Since the throwout factor is appropriately 0.5 and the resolution width is 5000 sec.$^{-1}$, a spectrum 1 Mc/sec. wide will result in an average reduction in beam intensity of approximately 0.2 percent. In the course of the experiments changes as small as 0.1 percent were measured. Therefore, the oscillator and the detector were isolated to the extent that the oscillator impulse on switching was less than 0.1 percent of the total signal. However, the fluctuations of individual readings, caused by unsteadiness of the beam, were sufficiently large to require the average of four readings for each experimental point.

III. EXPERIMENTAL RESULTS

In an unpublished experiment performed in February, 1939, Kusch and Millman, while investigating the g-factors of Br^{79} and Br^{81}, found a broad and unexplained series of resonances in NaBr. The present experiments result from a further study of this phenomenon.

Figure 2 is the spectrum of NaBr observed at

2733. gausses (approximately the field values used in the previous experiments). The spectrum is essentially the same in detail as that observed by Millman and Kusch, with the principal difference being the use of the variable frequency and fixed field. The chief features of the spectrum are the broad central minimum (of width about 0.35 Mc/sec.), the large total extent of the spectrum (about 1.2 Mc/sec.), and the appearance of other subsidiary minima. As a reference, the frequency at which an uncoupled Na^{23} nucleus ($g=+1.4765 \pm 0.0015$ nuclear magnetons)[7] would show a resonance minimum at the same field, is shown on the figure. It is observed to be roughly in the center of the spectrum. The obvious next step is to observe the same spectrum at approximately double the field strength. Figure 3 shows the results for a field of 5507. gausses. A simplification in the spectrum is discernible. The central minimum is approximately half the width and twice as deep and still shows the same structure which has the appearance of two unresolved

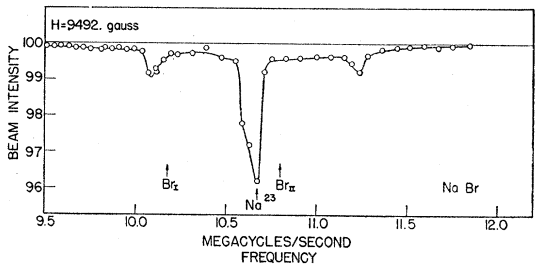

FIG. 4. Radiofrequency spectrum of NaBr at approximately double the field of Fig. 3 and 4-amperes radiofrequency current. There are no features that are different from those observed in Fig. 3, but again the central minimum is deeper and narrower. The additional arrows indicate the resonance positions of the two bromine isotopes that are not observed in this spectrum.

minima. There are two plateaus which terminate in lesser minima at approximately 0.6 Mc/sec. on either side of the central minimum. These subsidiary minima cut off sharply into residual plateaus which are 0.002 deep and which extend for 0.5 Mc/sec. on either side of the spectrum. Finally, Fig. 4 is the spectrum at approximately double the field (9492. gausses) for that of Fig. 3, and it is clear that aside from the central minimum becoming twice as deep and one-half again as narrow, there is no significant difference between this spectrum and that of Fig. 3. Apparently, the low frequency minimum of the pair composing the central minimum in Figs. 2 and 3 has been submerged in Fig. 4. In order to study the detail of the central minimum (For the sake of completeness, a run (Fig. 5) was taken at one-half the field value (1367. gausses) of Fig. 2. The complete deterioration of the pattern is clear. There is a mass of structure that shows very little characteristic feature.), its spectrum was repeated at lower radiofrequency current and correspondingly smaller intervals. Figure 6 is the curve. The general features are the same. In particular, the upper frequency side shows a very sharp cut-off.

These first results offer some immediate conclusions. Inasmuch as the average frequency of the observed spectrum is proportional to the field, the spectrum must be associated with some effective magnetic moment. That this moment is that of Na^{23} is clear from the close agreement of the resonant frequency of the Na^{23} nucleus and the position of the sharp central minimum in Fig. 4. They agree to 0.2 percent, which is within the experimental error. The resonant frequencies for Br^{79} and Br^{81} are also shown in Fig. 4. No evidence of these resonances exists in NaBr. This is undoubtedly due to the low intensity of the effect for bromine.[8] The frequencies of the side minima are not proportional to the field but remain at a constant frequency difference from the central minimum. This implies some orientation-dependent interaction

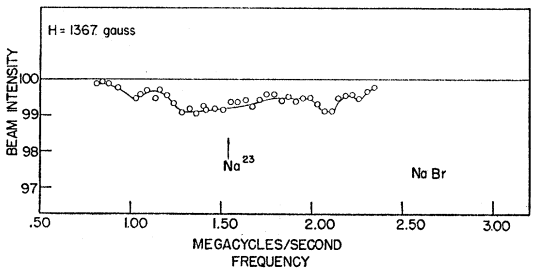

FIG. 5. Radiofrequency spectrum of NaBr at approximately one-half the field of Fig. 2. At this field the orientation-dependent interaction of the Na^{23} nucleus with the external field is approximately equal to its orientation-dependent interaction with the molecule. Note the complete degeneracy of the spectrum (compare Figs. 2, 3, and 4).

[7] S. Millman and P. Kusch, Phys. Rev. **60**, 91 (1941).

[8] S. B. Brody, W. A. Nierenberg, and N. F. Ramsey, Phys. Rev. **72**, 258 (1947).

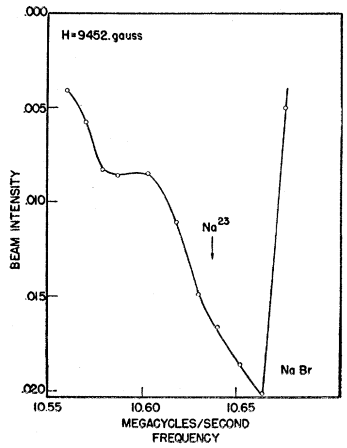

FIG. 6. Detail of the central minimum of the radiofrequency spectrum of NaBr at greater resolution. The field is approximately the same as for Fig. 4 but the radiofrequency current is one ampere, corresponding to the best resolution of the apparatus for this g-factor. Note the sharp asymmetry. The maximum reduction in intensity is one-half that for Fig. 4. This is in good agreement with the theory which predicts a variation of the maximum reduction in intensity proportional to the square root of the radiofrequency current in this region.

between the nucleus and the rest of the molecule in addition to the interaction between the nucleus and the external field. If this be so, it can be expected that NaCl and NaI would show similar spectra under approximately the same conditions. Figures 7 and 8 are the spectra of NaCl and NaI at fields corresponding to NaBr in Fig. 4. The general features of the spectra are the same. The frequency difference between the side minima of NaBr is greater than that for NaI and less than that for NaCl. The low plateaus beyond the side minima were not directly investigated for NaCl and NaBr because the effect is so close to the noise level. However, in a separate experiment at greater radiofrequency current the existence of the plateaus was confirmed for NaCl.

In addition to these spectra which were observed at such values of the field that the interaction of the Na^{23} magnetic moment with the field is comparable with, or larger than, the internal interaction, a type of spectrum new to molecular-beam research was undertaken. Observations were made at fields such that the nuclear interaction with the field is small compared to the orientation dependent interaction with the molecule. The most important case occurs when the field is nearly zero. (The demagnetization procedure is such that the field is 4 gausses or less.) There is some *a priori* question of the feasibility of such experiments because the absence of a homogeneous field allows non-adiabatic transitions of the molecules undergoing the abrupt change in field on passing from the focusing field to the low field region and on to the refocusing field. The fact that a spectrum is observed is sufficient proof that all the molecules do not undergo non-adiabatic transitions, and the remainder are responsible for the observed spectra. Figures 9–11 are the spectra of NaBr, NaI, and NaCl, respectively, at fields that are less than 4 gausses. One minimum is observed for each substance, and the center of each minimum corresponds very closely in frequency with the difference in frequency between the side minima of the corresponding strong-field spectra. The three spectra agree in general detail. They are broad (0.15–0.20 Mc/sec. in half-width) and they are asymmetrical. The upper frequency side rises more sharply than the lower frequency side.

While it is clear that the zero-field spectra will be of primary importance in the discussion, it is instructive to examine the behavior of the pattern in weak fields. Figures 12 and 13 are the spectra for NaBr at fields of 139 and 282 gausses, respectively. At these low fields there is considerable uncertainty in values of the field ($\sim$5 percent). Experimentally these spectra are the connection between the zero-field spectra and the intermediate- and strong-field spectra of NaBr. Figures 2–5, 9, 12, and 13 show the radiofrequency spectrum associated with Na^{23} in NaBr over a wide range of magnetic fields. Without a suitable theory of the interaction responsible for the zero-field minimum, it is

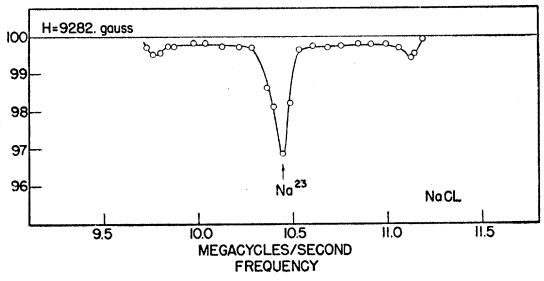

FIG. 7. Radiofrequency spectrum of NaCl at the strongest field available and radiofrequency current at 10 amperes (compare Fig. 4).

difficult to discuss Figs. 12 and 13 in any general way. However, it can be observed that the spectrum is broadened roughly proportionally to the field, and, in particular, the stronger field shows three resolved minima. Further discussion of the weak-field spectra will be given in Section VI.

IV. GENERAL DISCUSSION

One problem of this paper is to find the correct interaction between the nucleus in question and the remainder of the molecule to explain the observed spectra. The usual Hamiltonian for the orientation-dependent nuclear interactions assumed for a rotating diatomic molecules in a $^1\Sigma$ state[2,4] is

$$\begin{aligned}\mathcal{H} = &-g_1\mu_N \mathbf{I}_1\cdot\mathbf{H} - g_2\mu_N \mathbf{I}_2\cdot\mathbf{H} - g_J\mu_N \mathbf{J}\cdot\mathbf{H}\\ &-g_1\mu_N H_1'\mathbf{I}_1\cdot\mathbf{J} - g_2\mu_N H_2'\mathbf{I}_2\cdot\mathbf{J}\\ &+(g_1g_2\mu_N^2/r_J^3)[\mathbf{I}_1\cdot\mathbf{I}_2 - 3(\mathbf{I}_1\cdot\mathbf{r}_J)(\mathbf{I}_2\cdot\mathbf{r}_J)/r_J^2]\\ &+\sum_{i=1,2} e^2q_iQ_i/2J(2J-1)I_i(2I_i-1)\\ &\times[3(\mathbf{I}_i\cdot\mathbf{J})^2+\tfrac{3}{2}(\mathbf{I}_i\cdot\mathbf{J})\\ &\qquad -I_i(I_i+1)J(J+1)]. \quad (1)\end{aligned}$$

μ_N is the nuclear magneton, H is the external magnetic field, J the rotational angular momentum, I is the nuclear spin and g the corresponding g-factor. The quantity r_J is the internuclear distance, Q the quadrupole moment of the nucleus defined[4] as $eQ=\int(3z^2-r_1^2)de$, and q is defined by $eq=\int(3\cos^2\theta-1)/r_e^3de$, where the integral is carried over all charges in the molecule outside of a small sphere containing the nucleus for the rotational state $J_z=J$. H' is the magnetic field at the position of the nucleus caused by the molecular rotation. The first two terms of the Hamiltonian represent the interaction of the nuclear magnetic moments with the external field. This interaction corresponds to a frequency of 0.76 Mc/sec. for $g_i=1$ in an external field of 1000 gausses. The third term is the interaction of the magnetic moment of the rotation of the molecule with the external field. This term would have an estimated $g_J=0.1$. However, in strong fields the transitions observed correspond to $\Delta m_J=0$, and therefore this term contributes nothing to the spectrum. The fourth and fifth terms are the interactions of the nuclear moments with the field at the nuclei caused by the rotation of the molecule. This field can be estimated by considering the other nucleus and surrounding electrons as one electron charge rotating about the nucleus in question and causing an estimated frequency difference of $4g_I\mu_N^2/hr_J^3$ for an average value $J=40$. If $r_J=2.5\times10^{-8}$ cm (a good assumption for most diatomic molecules), then the corresponding frequency is 1000 cycles/sec. As discussed in Section VI, this estimate of the $\mathbf{I}\cdot\mathbf{J}$ interaction is too naive and must be replaced by more detailed consideration of the rotation. Similarly, the sixth term, the dipole-dipole interaction of the two nuclei, is of the same order. Finally, the

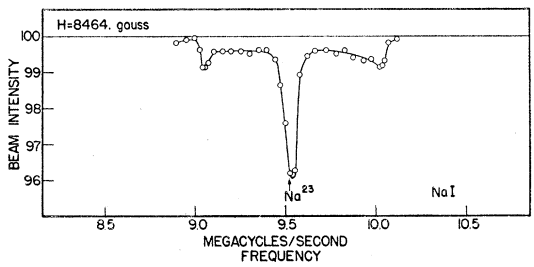

FIG. 8. Radiofrequency spectrum of NaI at the strongest field available and radiofrequency current at 10 amperes (compare Fig. 4).

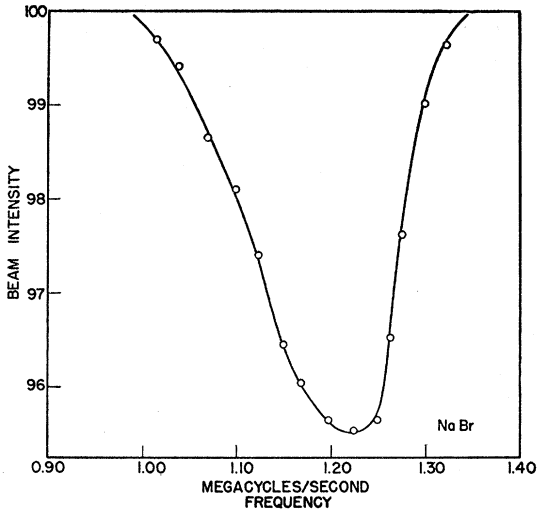

FIG. 9. "Zero"-field radiofrequency spectrum of NaBr. The radiofrequency current is 3 amperes. This spectrum is essentially due to the interaction of the nucleus with the molecule only. Note that the position of the minimum is almost exactly at a frequency equal to the difference between frequencies of the side minima of Fig. 4. The width is much larger than the natural width.

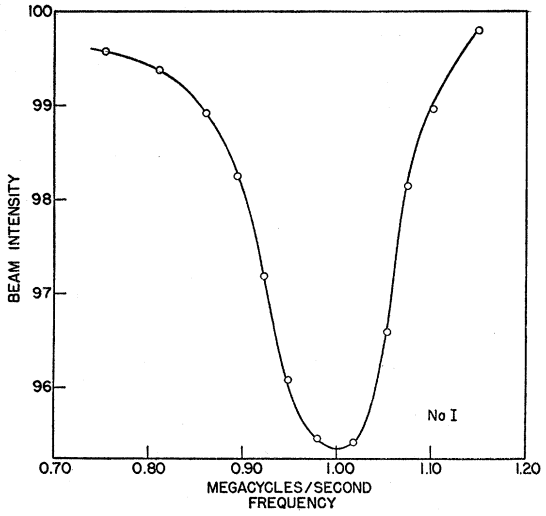

FIG. 10. "Zero"-field radiofrequency spectrum of NaI at 3-amperes radiofrequency current (compare Figs. 9 and 8).

last two terms represent the interaction of the quadrupole moments of the nuclei with the gradient of the electric field. This interaction is of the order of e^2Q/hr_J^3. If the quadrupole moment be taken as 10^{-25} cm^2, then for $r_J=2.5\times10^{-8}$ cm, the corresponding frequency is 0.23 Mc/sec.

In the HD and D_2 molecular-beam radiofrequency experiments,[2,4] all the minima observed were interpreted using the Hamiltonian of Eq. (1). The relative sizes of the interactions differ from the above estimates because of the small internuclear distance (10^{-8} cm) for D_2 and the small quadrupole moment of the deuteron (2.7×10^{-27} cm^2). The spectrum consisted of a series of discrete minima because the source was at liquid nitrogen temperature and therefore only the lowest rotational state contributed appreciably. The spectra reported here were observed under completely different experimental conditions. The dipole-dipole and the nuclear-rotation interactions are not observable because they are considerably less than the resolution of the apparatus (5000 sec.$^{-1}$). Therefore, these terms in the Hamiltonian may be neglected. For the typical sodium halide, the beam-source (oven) temperature is such that there are effectively 100 rotational states excited with the corresponding $2J+1$ values of J_z for each state. It is clear then that the strong-field spectrum will not, in general, be a series of discrete peaks whose width is the resolution width, but, instead, will be a continuum whose extent in frequency will be measured by the largest internal interaction. Assuming the estimates made above to be valid, a sufficiently large quadrupole interaction of Na^{23} in the sodium halides will be assumed.

A statistical theory of the effect of a nuclear-electrical quadrupole moment in the molecular-beam radiofrequency spectrum, including the contribution to the Hamiltonian of the rotational magnetic moment has been developed by Feld and Lamb.[9] Figure 14 is a copy of their Fig. 5, redrawn to show the spectrum as a reduction in beam intensity. The assumptions and approximations that were made in arriving at Fig. 14 are the following: (1) The nuclear spine in $\frac{3}{2}$, (2) The rotational angular momentum $J\gg1$, (3) H is large, so that $\mu_N g_i H\gg e^2qQ/4$. (4) The central minimum is drawn in arbitrary fashion to correspond to the resolution width of the apparatus. (This minimum, corresponding to a nuclear reorientation $m_I=\frac{1}{2}\leftrightarrow m_I=-\frac{1}{2}$, shows no quadrupole effect to the first order in the perturbation calculation.) (5) The spectrum is calculated as the product of the density of transitions in energy and the transition probability. The actual depths of the minima are determined by the resolution of the apparatus. This approximation is very

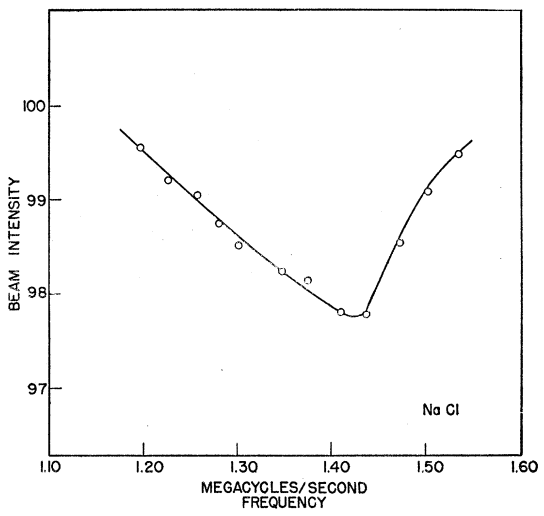

FIG. 11. "Zero"-field radiofrequency spectrum of NaCl at 3 amperes (compare Figs. 9 and 7).

[9] B. T. Feld and W. E. Lamb, Jr., Phys. Rev. 67, 15 (1945).

good. (6) The other nucleus has spin zero. It is assumed that the results for the strong-field spectra of the sodium halides will be unaffected by the spin of the halogens concerned. In the case of homonuclear molecules such as Na_2, there is a definite effect of the spins of both nuclei which has been calculated by H. M. Foley.[10]

The spectra of Figs. 4, 7, and 8, were observed under conditions suitable for comparison with Fig. 14 (the largest fields available). The value of $e^2qQ/4\mu_N gH$ is approximately 0.05 for each. The general agreement with the theory is very good. There are three minima with the central minimum corresponding to the Larmor frequency of the Na nucleus. The side minima cut off relatively sharply into the side plateaus which the theory also predicts. When these experiments were performed the g-values of Br^{79} and Br^{81} were not known. They have since been measured,[8] and their spectra do fall within the spectrum of Fig. 4. (A careful search for these minima confirmed their absence and the cause is undoubtedly lack of intensity.) The Cl^{35} and Cl^{37} resonances are far removed from the Na resonance and the I^{127} g-factor is still unknown. Figure 14 shows that $e^2qQ/2h$ can be estimated from the actual spectrum as the frequency difference of the side minima.

In the absence of an external field, and assuming a negligible contribution from the halide nucleus in first approximation, the Hamiltonian of Eq. (1) will consist of one term, the quadrupole interaction of the Na nucleus. The energy levels have been computed by Feld and Lamb,[9] and the only non-vanishing transition is at a frequency $e^2qQ/2h$. The zero-field spectra were observed at these frequencies (Figs. 9, 10, 11).

Table I gives the comparison of $e^2qQ/2h$ obtained from the strong-field and the zero-field spectra. They agree to better than 5 percent. However, the differences are systematic, the weak-field values being the larger, and the differences are beyond experimental error. This difference is not yet explained. An estimate of $e^2qQ/2h=0.13$ Mc/sec. (corrected for resolution) has been made from the strong-field spectrum of Na_2^{23} reported by Millman and Kusch. In this case, the theory of Lamb and Feld does not apply because of spin degeneracy. Foley[10] has developed the correct theory for homonuclear diatomic molecules, which is the basis of the above estimate.

[10] H. M. Foley, Phys. Rev. 71, 747 (1947).

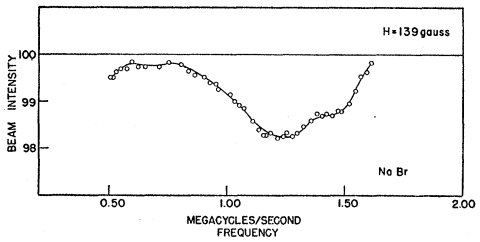

FIG. 12. Radiofrequency spectrum of NaBr in weak fields. The interaction of the Na^{23} nucleus with the external field is less than the orientation-dependent interaction of the nucleus with the molecule. Note that the spectrum is broadened but still situated about the central frequency of Fig. 9.

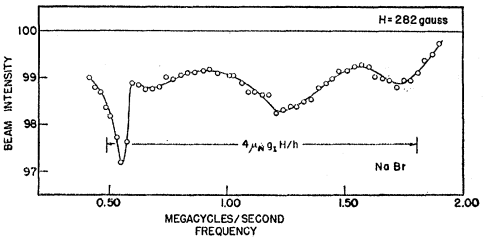

FIG. 13. Radiofrequency spectrum of NaBr in a field approximately double that of Fig. 12. The spectrum is broadened approximately proportionately to the field and still is approximately centered about the central frequency of Fig. 9. Three minima are observed in agreement with theory. $4\mu_N g_I H/h$ is calculated equal to 1.3 Mc/sec., and compared with the separation of the outer minima. Again there is approximate agreement with experiment.

Feld and Lamb also discuss the Zeeman broadening of the zero-field line. The theory predicts a broadening of the line proportional to $\mu_N g_I H$. It also predicts a possible resolution into three minima. Figures 12 and 13 are the actual spectra for weak fields. The broadening of the zero-field lines is clearly proportional to the fields, and for the stronger field (Fig. 13) three minima are actually observed. The frequency difference between the three extreme peaks is less than the predicted value of $4\mu_N g_I H/h$ by 10 percent. The discrepancy is due in part to poor field calibration at low fields and in part to the fact that at this value of the field the magnetic interaction is not small compared to the internal interaction, and hence the first-order theory cannot be expected to give very accurate results.

The conclusion to be drawn from this general discussion is that the radiofrequency spectrum

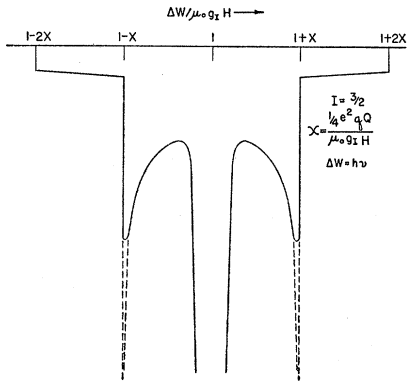

FIG. 14. This is a copy of Fig. 5 from Feld and Lamb's paper.[9] This is the predicted radiofrequency spectrum of a nucleus of spin $\frac{3}{2}$ in a diatomic molecule, where an electrical-quadrupole interaction with the molecule is assumed but is very small compared to the interaction of the nucleus with the external magnetic field. The ordinate is proportional to the beam intensity, the abscissa is a dimensionless frequency.

of the Na halides is to be explained in gross detail on the assumption of a sufficiently large nuclear-electric quadrupole interaction of about 1 Mc/sec. The succeeding sections of this paper are devoted to an analysis of the finer details to ascertain the limits of application of the theory and the completeness of the Hamiltonian of Eq. (1). The width of the central minimum in strong fields as a function of the field is explained on the basis of a quadrupole interaction. The effect of the finite resolution of the apparatus and the finiteness of J are introduced into the theory and compared with observation. These are found to be insufficient to explain all the detail observed, and a term $-c\mathbf{I}\cdot\mathbf{J}$ is added to the Hamiltonian to explain this insufficiency.

V. ANALYSIS OF HIGH FIELD RESULTS

The frequency differences of a nucleus in a strong magnetic field are, from the Hamiltonian of Eq. (1), including only the first and last terms for one nucleus of spin $\frac{3}{2}$, to second order in x_0,

$$\bar{\nu}(\tfrac{3}{2},\tfrac{1}{2})/\nu_I=1-x_0[1-3(1-1/J)z^2]+6x_0^2z^2(1-z^2). \quad (2a)$$

$$\bar{\nu}(\tfrac{1}{2},-\tfrac{1}{2})/\nu_I=1-\tfrac{3}{4}x_0^2[(1-z^2)(9z^2-1)]-(3x_0^2/2J)(9z^4-5z^2), \quad (2b)$$

$$\bar{\nu}(-\tfrac{1}{2},-\tfrac{3}{2})/\nu_I=1+x_0[1-3(1-1/J)z^2]+6x_0^2z^2(1-z^2). \quad (2c)$$

The matrix elements of the Hamiltonian giving rise to these frequency differences are explicitly calculated by Kellogg, Rabi, Ramsey, and Zacharias.[4] The expressions for the transition frequencies are expanded to the first term in $1/J$. $\bar{\nu}(m_I, m_I-1)$ is the frequency observed in the transition $m_I-1\rightarrow m_I$. ν_I is the Larmor frequency $\mu_N g_I H/h$; z is the cosine of the angle between J and H (J large) or $z=m_J/J$; $x_0=e^2q'Q/4\mu_N g_I H$; $q=-2Jq'/2J+3$ and q' is independent[11] of J. For J large, $q'=-q$. These equations are similar to those derived by Feld and Lamb. The only difference is the expansion to the first power in $1/J$. The $1/J$ terms are included only for the leading term in the perturbation series with respect to x_0. Figure 14 was calculated from these equations neglecting second-order terms in x_0 and the terms in $1/J$. The quantity actually plotted was the product of the density of transitions $dz/d\bar{\nu}$ and the transition probability for small perturbations of the oscillating field. In the experiments reported here the oscillating field is not a small perturbation, since a large fraction of the molecules capable of undergoing transitions actually do so, although all are not observable because of lack of perfect defocusing, but the transition probabilities are independent of z in strong field and hence the complete spectrum will retain its symmetry although the strengths of the various minima will differ. This is not true for the weak-field experiments and therefore the spectrum in this case is considerably less than ideal.

The central minimum of Figs. 3–5 corresponds to the transition $m_I=\frac{1}{2}\leftrightarrow-\frac{1}{2}$ because the term in x_0 vanishes for that transition. The widths of the observed central minimum at different fields are due to the effect of the term in x_0^2. Figure

TABLE I. Comparison of weak-field and strong-field interactions.

Substance	External magnetic field (gausses)	$e^2qQ/2h$ (Mc/sec.)
NaBr	9490	1.17
NaBr	4	1.22
NaCl	9282	1.35
NaCl	4	1.42
NaI	8494	0.97
NaI	4	0.99

[11] A. Nordsieck, Phys. Rev. **58**, 310 (1940).

15a is the theoretical plot of $\bar{\nu}/\nu_I$ *versus* z, neglecting terms of order $1/J$. There are two extremes which define the limits of $\bar{\nu}/\nu_I$. Here z is a multi-valued function of $\bar{\nu}/\nu_I$, and therefore the density of transitions is computed as $|dz_1/d\bar{\nu}|+|dz_2/d\bar{\nu}|$ *versus* z. Figure 15b is the plot of the density of transition, omitting the $1/J$ terms. The two extremes are represented here as two peaks separated in frequency by $25x_0^2\nu_I/12$. The corresponding minima were actually observed in Figs. 3 and 4. The lower frequency minimum is the more prominent, judging from the area underneath the associated peak in Fig. 15b. The observed widths are also in good agreement with the theory. The quantity $2x_0\nu_I$ is the separation of the subsidiary minima. Using the values of x_0 from the curves at different fields, we construct Table II, which compares the widths of the central minima for various fields *versus* $25x_0^2\nu_I/12$. The width of the minimum for 9500 gausses is taken from Fig. 6 rather than from Fig. 4 because of the increased broadening by the radiofrequency current. The agreement is again good within the chief approximation still to be considered; namely, the effect of the finite resolving power of the apparatus. This is responsible for the systematic deviations in Table II. However, aside from this difference, the widths of the central minima are inversely proportional to the field.

This theory of the structure of the central minimum is important when considered from the viewpoint of the precision measurement of nuclear magnetic moments. The quadrupole moment introduces asymmetries which are proportional to the square of the ratio of the quadrupole and the magnetic interactions. If the center of the minimum is used, a fractional error proportional to x_0^2 is introduced in the measurement of the nuclear g for half-integral

TABLE II. Comparison of the half-widths of the central minimum with theory for NaBr.

Field (gausses)	x_0	$(25/12)x_0^2\nu_I$ (Mc/sec.)	Measured half-width Mc/sec.
9452	0.055	0.07	0.08
5507	0.094	0.11	0.16
2733	0.187	0.22	0.31

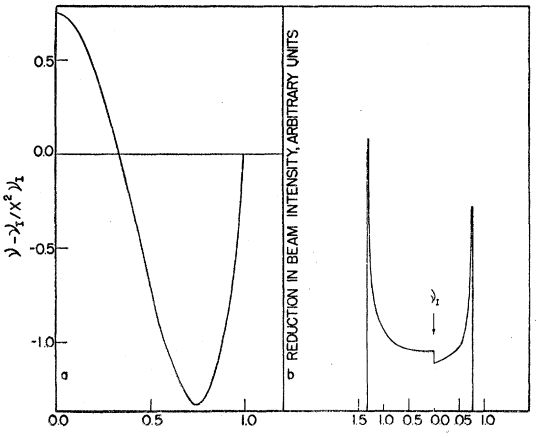

FIG. 15. Theoretical shape of the central minimum in strong fields. ν is the transition frequency between levels, and ν_I is the Larmor frequency for the nucleus. Figure 15a is, therefore, a plot of the reduced frequency difference $\nu/\nu_I/x^2\nu_I$ *versus* z, the cosine of the angle between J and H for $J\gg1$. Using this function, the line shape, uncorrected for finite resolution, is plotted in 15b as a reduction in beam intensity *versus* the reduced frequency difference. Note that the two peaks correspond to the two stationary points of Fig. 15a (compare Figs. 2 and 3).

spin. If the spin is $\frac{3}{2}$, this yields an underestimate $7x_0^2/24$. The error that would be made in measurement of the value of g for Na^{23} from Fig. 4 is 0.1 percent. In Figs. 2–4 and 6 the position of the Na^{23} resonance frequency is indicated, and its relative position is correct within the precision of the measurement of the field. It should be noted that these asymmetries are proportional to the square of the perturbation parameter and therefore independent of the sign of the quadrupole moment.

At still lower values of the field, Fig. 5 (where $x_0=0.4$), the central minimum has practically disappeared. The entire structure becomes complicated. In fact, for $x=0.5$, additional minima are predicted. Despite the increasing complexity of the spectrum, the over-all width remains the same. This is due to the vanishing of the second-order terms for $z=0$ in Eqs. (2a) and (2c). The positions of the side minima are therefore unaffected by the second-order perturbation term. This has two effects: the width of the spectrum remains constant over a very wide range of x_0 (experimentally, down to 0.5 where the weak-field representation is the more appropriate) and it prevents the determination of the sign of the quadrupole interaction from this statistical data.

Comparison of the experiments with theory disclosed one discrepancy. The values for $e^2qQ/2h$ obtained from the zero-field data were approximately 5 percent greater than those obtained from the strong-field data. A possible explanation of this difference is the effect of the resolution of the apparatus. The theory until now has neglected the effect of the apparatus resolution, with the result that the minima observed experimentally in strong fields are infinite in the theory. The finite resolving power of the apparatus will cut off these minima and shift their positions. The shape of the resonance curve for a single level is given by[12]

$$P_{\frac{1}{2},-\frac{1}{2}}=[\Delta^2/(1-q)^2+\Delta^2]\times\sin^2\pi ft[(1-q)^2+\Delta^2]^{\frac{1}{2}}. \quad (3)$$

$\Delta=H_1/2H_0$, one-half the ratio of the amplitudes of the oscillating and static fields, q is the ratio of the applied to the resonant frequency, f is the applied frequency, and t is the time interval the system has been in the magnetic field. The Rabi formula has the usual resonance denominator, but, since the resolution widths are different for different molecular velocities and the narrowest structure to be interpreted is ten times this average width, it is sufficiently representative to choose this function as

$$F(\bar{\nu},\nu)=K_1K_2, \quad \nu-\Delta\bar{\nu}\leqslant\bar{\nu}\leqslant\nu+\Delta\bar{\nu}, \quad (4)$$

and $F(\bar{\nu},\nu)=0$ for all other values of $\bar{\nu}$. $\Delta\bar{\nu}$ is half the resolution width and is to be estimated in a particular case from Eq. (3). K_1 is a factor introduced to compensate for the lack of complete defocusing of the apparatus. K_2 is introduced to compensate for the different final magnetic states of the nucleus caused by the spread in times t that (Eq. (3)) the various molecules of the Maxwellian beam spend in the oscillating field. Both K_1 and K_2 are less than unity. The method of calculation of the line shape for the transitions $m_I=\frac{3}{2}\leftrightarrow\frac{1}{2}$ and $m_I=\frac{3}{2}\leftrightarrow\frac{1}{2}$, including the effect of the resolution and the term in $1/J$, is outlined in Appendix I (Eqs. (14), (15), and (16)). The result is

$$R(\nu)=\frac{K_1K_2}{3(3x_0\nu_I)^{\frac{1}{2}}}[\nu+\Delta\bar{\nu}-(1-x_0)\nu_I]^{\frac{1}{2}}\times(1+a\tfrac{1}{2}\sqrt{\pi}),\quad (1-x_0)\nu_I-\Delta\bar{\nu}\leqslant\nu\leqslant(1-x_0)\nu_I+\Delta\bar{\nu},$$
$$R(\nu)=\frac{K_1K_2}{3(3x_0\nu_I)^{\frac{1}{2}}}\{[\nu+\Delta\bar{\nu}-(1-x_0)\nu_I]^{\frac{1}{2}}-[\nu-\Delta\bar{\nu}-(1-x_0)\nu_I]^{\frac{1}{2}}\}(1+a\tfrac{1}{2}\sqrt{\pi}),\quad \nu\geqslant(1-x_0)\nu_I+\Delta\bar{\nu}. \quad (5a)$$

$$R(\nu)=\frac{K_1K_2}{3(3x_0\nu_I)^{\frac{1}{2}}}[(1+x_0)\nu_I-\nu+\Delta\bar{\nu}]^{\frac{1}{2}}(1+a\tfrac{1}{2}\sqrt{\pi}),\quad (1+x_0)\nu_I-\Delta\bar{\nu}\leqslant\nu\leqslant(1+x_0)\nu_I+\Delta\bar{\nu},$$
$$R(\nu)=\frac{K_1K_2}{3(3x_0\nu_I)^{\frac{1}{2}}}\{[(1+x_0)\nu_I-\nu+\Delta\bar{\nu}]^{\frac{1}{2}}-[(1+x_0)\nu_I-\nu-\Delta\bar{\nu}]^{\frac{1}{2}}\}(1+a\tfrac{1}{2}\sqrt{\pi}),\quad (1+x_0)\nu_I-\Delta\bar{\nu}\geqslant\nu. \quad (5b)$$

Equation (5a) is the spectrum of the transition $\frac{3}{2}\leftrightarrow\frac{1}{2}$. Equation (5b) is the spectrum of the transition $-\frac{3}{2}\leftrightarrow-\frac{1}{2}$. $R(\nu)$ is the fractional reduction in beam intensity or depth of resonance minima with respect to the total beam and

$$a^2=h^2/8\pi^2IkT=\pi/4\bar{J}^2,$$

where I is the moment of inertia of the molecule. The value of a is about 0.02. Examination of Eq. (5) shows that J finite but large (J affects Eq. (5) through a which is of the order of $1/J$) does not affect the position of the minima but increases the over-all reduction in beam intensity by ~ 2 percent. The maximum depth of resonance minima becomes $\frac{1}{3}K_1K_2[2\Delta\bar{\nu}/3x_0\nu_I]^{\frac{1}{2}}$ for both minima and occurs at frequencies $(1+x_0)\nu_I-\Delta\bar{\nu}$ and $(1-x_0)\nu_I+\Delta\bar{\nu}$. This is a difference between the minima of $2x_0\nu_I-2\Delta\bar{\nu}$. In the experiments at the strongest fields $2\Delta\bar{\nu}=0.02$ Mc/sec. This is in the right direction and accounts for approximately one-third of the discrepancy. The remainder is still beyond the experimental error (0.015 Mc/sec.). The experimental arrangement is such that $K_1=0.6$ and $K_2=0.5$. When applied to the experiment in the strongest field, this yields 0.011 for the fractional reduction in intensity at the side minima of NaBr, which compares

[12] I. I. Rabi, Phys. Rev. 51, 652 (1937).

well within the approximations to the observed value 0.012 if the value of $2\Delta\bar{\nu}$ is taken as 0.02 Mc/sec. The corresponding calculation for the central minimum is more tedious principally because of the averaging over J. However, it is not necessary to complete it for the points of major importance. Examination of Eq. (2b) shows that in the neighborhood of $z=0$ the term in $1/J$ vanishes $\sim z^2$, and therefore this term will have a negligible effect in broadening and lowering the higher frequency component of the central minimum. This minimum will be equal to $\frac{1}{3}K_1K_2[4\Delta\bar{\nu}/15x_0^2\nu_I]^{\frac{1}{2}}$ after averaging over the resolution (Appendix I). This gives a value of 0.03 which compares favorably with that of 0.04 observed (Fig. 4).

The reason for the experimental disappearance of the lower frequency component of the central minimum at the field of 9000 gausses is obscure. In principle the term in $1/J$ in Eq. (2b) could cause the necessary broadening of this minimum. However, the contribution of this term to the Hamiltonian vanishes at $z=(5/9)^{\frac{1}{2}}$, the value corresponding to this minimum. At this point in the discussion it is convenient to introduce the possibility of adding an additional term to the Hamiltonian to explain this broadening. Stronger arguments in favor of this additional interaction will be discussed later. For the present, it will only be noted that this interaction must satisfy the requirement that it submerge the lower frequency component of the central minimum at sufficiently strong fields. The simple operator $-c\mathbf{I}\cdot\mathbf{J}$ satisfies this condition. If this term be added to the Hamiltonian, then in strong fields the equation equivalent to (2b) becomes (Appendix II, Eq. (20))

$$\bar{\nu}(\tfrac{1}{2},-\tfrac{1}{2})/\nu_I=1-\tfrac{3}{4}x_0^2[(1-z^2)(9z^2-1)] +yz+\tfrac{1}{2}y^2(1-z^2), \quad (6)$$

where, for convenience, the dimensionless parameter $y=cJ/\mu_N g_I H$ is introduced. The calculation is to the second order in x_0 and y. To fix ideas, at a field $H=10{,}000$ gausses, $x_0\cong 0.05$, and y will be assumed $\cong 0.005$, which is equivalent to an average ($J=40$) $cJ/h=0.05$ Mc/sec. If $y=0$, Eq. (6) reduces to Eq. (2) (neglecting terms of order $1/J$). Just as before, values of $\bar{\nu}$ are sought for which $d\bar{\nu}/dz$ vanishes. The result, to sufficient approximation, is

$$\bar{\nu}/\nu_I=1+3x_0^2/4+y^2/30x_0^2. \quad (7a)$$

$$\bar{\nu}/\nu_I=1-4x_0^2/3-y^2/30x_0^2+(5/9)^{\frac{1}{2}}y. \quad (7b)$$
$$\bar{\nu}/\nu_I=1-4x_0^2/3-y^2/30x_0^2-(5/9)^{\frac{1}{2}}y.$$

If $y=0$, there are but two distinct values, corresponding to the two minima in Fig. 15. The effect of the additional interaction is to shift the position of the minima in frequency by $(y^2/30x_0^2)\nu_I$ and to split the lower frequency minimum into two minima whose separation is $2(5/9)^{\frac{1}{2}}y\nu_I$. $(y^2/30x_0^2)\nu_I\cong 3000$ sec.$^{-1}$ which is less than the resolution width of the apparatus and therefore not observable. Hence the higher frequency minimum will remain sharp. The lower frequency minimum will be broadened by an amount equal to the separation of its two components for an average value of J. For the values of the interaction cited, the corresponding width is 0.07 Mc/sec. or of the same magnitude as the x_0^2 broadening. The splitting, as such, is not observable, because the position of the lines are still to be averaged over J. The net result of the $\mathbf{I}\cdot\mathbf{J}$ interaction is to submerge the lower frequency minimum at a field $H=10{,}000$ gausses. At appreciably smaller values of the field (5000 gausses), the relative effect of this term on the lower component disappears. The addition of this term will have a negligible effect on the spectrum corresponding to the transitions $\pm\frac{3}{2}\leftrightarrow\pm\frac{1}{2}$, because it is small compared to the first order terms in x_0.

VI. ANALYSIS OF WEAK-FIELD RESULTS

In a weak field the chief unexplained feature is the anomalous width of the lines ($\sim$0.15 Mc/sec.). The Hamiltonian for the quadrupole interaction in zero fields is (from Eq. (1))

$$\mathcal{H}=\frac{e^2qQ}{2J(2J-1)I(2I-1)}\{3(\mathbf{I}\cdot\mathbf{J})^2 +\tfrac{3}{2}(\mathbf{I}\cdot\mathbf{J})-I(I+1)J(J+1)\}, \quad (8a)$$

and the energy levels are given by[13]

$$W_F=\frac{e^2qQ}{2J(2J-1)I(2I-1)}\{\tfrac{3}{4}K^2+\tfrac{3}{4}K -I(I+1)J(J+1)\}, \quad (8b)$$

[13] H. B. G. Casimir, *On the Interaction Between Atomic Nuclei and Electrons* (Teyler's Tweede Genootshap., 1936).

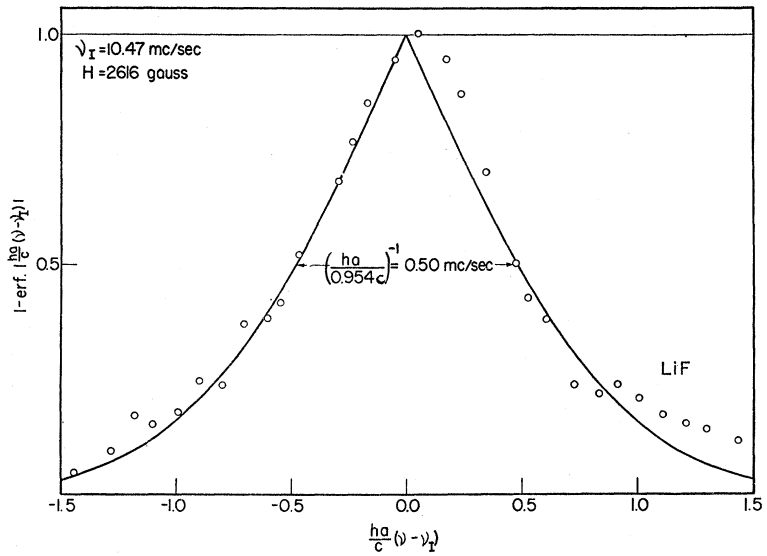

FIG. 16. Comparison of theory and experiment for the radio-frequency spectrum of LiF. The experimental points are plotted as reduction in beam intensity (normalized to unity for the maximum) *versus* the difference in frequency from the Larmor frequency for fluorine normalized by the factor $ha/c=1.91\times10^6$ sec. The solid line is the calculated line shape for a total orientation-dependent Hamiltonian, equal to $-\mu_N g_I \mathbf{I}\cdot\mathbf{H}-c\mathbf{I}\cdot\mathbf{J}$.

where

$$K=F(F+1)-I(I+I)-J(J+1)$$

and $F=J+i$ and $i=I,\ I-1,\ \cdots,\ -I$. For J infinite and $I=\frac{3}{2}$ the energy differences are given by

$$\begin{aligned} W_{3/2}-W_{\frac{1}{2}}&=e^2qQ/2,\\ W_{\frac{1}{2}}-W_{-\frac{1}{2}}&=0,\\ W_{-\frac{1}{2}}-W_{-3/2}&=-e^2qQ/2. \end{aligned} \tag{9}$$

For J finite, the level differences are

$$\begin{aligned} W_{3/2}-W_{\frac{1}{2}}&=-e^2q'Q/2,\\ W_{\frac{1}{2}}-W_{-\frac{1}{2}}&=\frac{3e^2q'Q}{2}\,\frac{2J+1}{(2J-1)(2J+3)}\\ &\cong 3e^2q'Q/4J, \end{aligned} \tag{10}$$

$$W_{-\frac{1}{2}}-W_{-3/2}=e^2q'Q/2.$$

(Note the introduction of q', as in Eq. (2) which is independent of J.) The result is that the line at $\nu=e^2q'Q/2h$ is completely unaffected by the distribution of rotational states when $I=\frac{3}{2}$. The spectrum due to $W_{\frac{1}{2}}-W_{-\frac{1}{2}}$ is not observable because of the presence of non-adiabatic transitions near zero frequency.

In the preceding section the possibility of an interaction of the type $-c\mathbf{I}\cdot\mathbf{J}$, whose order of magnitude is $(cJ/h)_{Av}=0.05$ Mc/sec. was introduced. This term is diagonal in the same $\mathbf{F}=\mathbf{I}+\mathbf{J}$, M_F representation. (In fact any power series in $(\mathbf{I}\cdot\mathbf{J})$ is diagonal in this representation, and its set of eigenvalues is the series with the eigenvalues of $\mathbf{I}\cdot\mathbf{J}$ replacing $\mathbf{I}\cdot\mathbf{J}$ in the series.) In Appendix III (Eq. (23)) it is shown that the addition of this term to the Hamiltonian will cause a splitting and broadening of the zero-field peak with an over-all half-width equal to $2\pi^{-\frac{1}{2}}2.64(cJ/h)_{Av}$ or 0.15 Mc/sec. This value is in good agreement with experiment, but there was no resolution into twin lines. This is not a fundamental difficulty because the effect of the first few excited vibrational states and of the centrifugal expansion of the rotating molecule on q' can easily be such as to smear out the structure and produce the observed asymmetries.

The splitting of the zero-field lines, Figs. 12 and 13, are not in as clear agreement with theory. It will be recalled that the frequency difference between the extreme minima was 10 percent too low, and there was lack of symmetry about the center of the spectrum. The reasons are probably several. The first is the uncertainty in the calibration of the field at low fields, the second the fact that the approximations used in the theory are not completely applicable. The perturbation introduced by the oscillating field is not small, and the only circumstance under which the Zeeman splitting is resolved (Fig. 13) is at a field where the perturbation of the fixed C-field is too large compared

to the quadrupole term and a more exact calculation would need to be made.

VII. GENERAL INTERACTIONS

Results similar to those found with the alkali halides and interpretable as quadrupole interactions are found in the spectra of other molecules. In fact, data of this nature were published by Millman and Kusch[5] prior to the development of the theory by Feld and Lamb. Examination of this data shows that the quadrupole interpretation is possible for Li_2^7 and K_2^{39} as well. The high spin and relatively narrow width of the Cs_2^{133} spectrum agree with the lack of structure observed. However, in no case do the halogens show structure that is easily interpretable as a quadrupole interaction. Cl^{35} and Cl^{37}, for example, show shallow, broad ($\sim$0.4 Mc/sec.), featureless resonances in NaCl. The radiofrequency spectrum of I^{127} has not yet been observed despite a number of searches, and this is presumably because of the extreme width of its spectrum.

A possible reason for this phenomenon can be inferred from the spectrum of F^{19}. F^{19}, having spin $\frac{1}{2}$ has no quadrupole moment, and therefore a quadrupole interaction is impossible. The sharpest F resonance observed, however, was reported by Millman and Kusch[3] for NaF where the half-width is 0.08 Mc/sec. The F resonance in CsF and LiF, however, reveal half-widths of about 0.5 Mc/sec. Fig. 16 is the plot of the relative change of beam intensity *versus* the relative difference in frequency from the Larmor frequency of a fluorine nucleus in LiF. An attempt to explain this width can be made by assuming an additional term in the Hamiltonian of the form $-c\mathbf{I}\cdot\mathbf{J}$, so that the Hamiltonian for F is therefore

$$\mathcal{H}=-\mu_N g_I \mathbf{H}\cdot\mathbf{I}-c\mathbf{I}\cdot\mathbf{J}. \qquad (11)$$

The additional term assumes a cosine coupling of the spin to the rotation which is proportional to the rotation. (The first power of the cosine operator is the maximum the symmetry of spin $\frac{1}{2}$ will allow.) This is similar in form to the operator for the interaction of the nuclear moment and the magnetic field because of the rotation of the molecular-charge distribution, but the order of magnitude assumed for c is greater. (The simpler interaction, $c\mathbf{I}\cdot\mathbf{J}/J$, whose strength is largely independent of the rotation, yields a result that is clearly not in agreement with experiment. The spectrum is rectangular with width $2c/h$.) In strong fields (Appendix III) the line-shape function derived from Eq. (11) is

$$dN/d\bar{\nu}=(ha\sqrt{\pi}/2c)\{1-\mathrm{erf}[(ha/c)\,|\,\bar{\nu}-\nu_I\,|\,]\}. \qquad (12)$$

The effect of resolution of the apparatus is not included in Eq. (12) because the large structure and absence of infinities make it relatively small. The solid curve of Fig. (16) is the theoretical curve computed from Eq. (12). The half-width of the line of Fig. 16 is 0.954 c/ha, and c/ha was evaluated by comparison with the observed value of 0.50 Mc/sec. Assuming an internuclear distance of 2.5A, the moment of inertia of the LiF molecule equals 52.6×10^{-40} g cm^2 and $a=2.57\times10^{-2}$ at the oven temperature of 1150°K. Therefore, $c=8.93\times10^{-23}$ erg and $c/g_I\mu_N$, the equivalent field at the nucleus per unit rotation, is 3.4 gausses in contrast to a value of 0.3 gauss per unit rotation to be, expected from a one-electron charge rotating at a distance of 2.5A from the F nucleus with the angular velocity of the molecule (Section IV).

The spectrum associated with Eq. (11) can be observed in weak fields. In Appendix III (Eq. 24) it is shown that the corresponding zero-field spectrum is

$$dN/d\bar{\nu}=2(ha/c)^2\bar{\nu}\exp[-(ha/c)^2\bar{\nu}^2]. \qquad (13)$$

The maximum R occurs at $\bar{\nu}=0.707c/ha$, and the spectrum has a half-width equal to 1.05

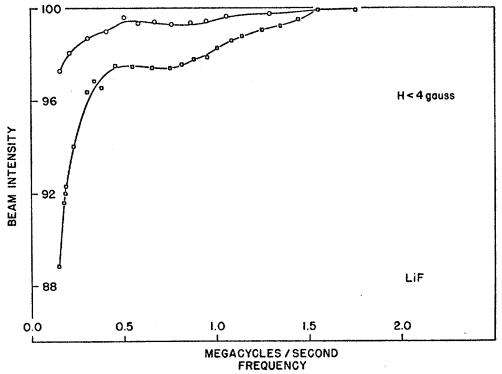

FIG. 17. "Zero"-field spectrum of LiF. The circled points correspond to a radiofrequency current of 3 amperes, and the squared points correspond to a radiofrequency current of 10 amperes.

c/ha. It is therefore broad. Figure 17 is the experimental weak-field spectrum. Qualitatively there is agreement. Unfortunately, the large fraction of the adiabatic transitions at near-zero frequency obscures the results. The expected minimum should be observed at 0.37 Mc/sec. Actually, it is observed at 0.7 ± 0.2 Mc/sec.

J. H. Van Vleck has offered the valuable suggestion that this cosine interaction may arise from second-order couplings between the nuclear spin and the electronic angular momenta even though the molecule is in a $^1\Sigma$ state. It is possible for such a second-order interaction also to introduce a quadrupole-like term. In this case the observed quadrupole interaction may be the sum of two parts: one attributable to a nuclear quadrupole moment and the other attributable to the second-order nuclear-electronic coupling. This effect and its probable magnitude are being further studied theoretically by J. H. Van Vleck and H. M. Foley. G. C. Wick is investigating this interaction using an approach similar to that adopted for the analogous interaction in H_2.[14,15]

This work has been facilitated by the contributions of present and past members of the molecular-beam laboratories. In particular, Professor I. I. Rabi suggested the initial line of research that led to the problem and also suggested the possibility of a cosine coupling of the nuclear spin to the rotational moment. Dr. S. Millman provided valuable advice in re-activating the apparatus. Drs. S. Brody and J. Trischka were of considerable help in the laboratory.

APPENDIX I. THE EFFECT OF THE FINITE RESOLUTION OF THE APPARATUS

Feld and Lamb have calculated the density of levels $|dz/d\bar{\nu}|$ for the transitions $\pm\frac{3}{2}\leftrightarrow\pm\frac{1}{2}$, using first-order perturbation terms. If $F(\bar{\nu},\nu)$ is there solution function for the apparatus (the specific one used is defined by Eq. (4)), then for a fixed but large value of J, the reduction in beam intensity at a frequency ν is given by

$$R(\nu,J)=\int_0^\infty F(\bar{\nu},\nu)\,|dz/d\bar{\nu}|\,d\bar{\nu} \tag{14}$$

if $dz/d\bar{\nu}$ nowhere changes sign. (In the problems considered $\bar{\nu}=f(z^2)$, and therefore the range of z is restricted to $0\leqslant z\leqslant 1$.) For the special function, F, chosen, (Eq. (4)) the spectral curve for any transition is

$$R(\nu,J)=(K_1K_2/2I)\,|z(\nu+\Delta\bar{\nu})-z(\nu-\Delta\bar{\nu})|. \tag{15}$$

This yields Eq. (5) with $a=0$. The coefficient $1/2I$ is an approximate normalization factor arising from the consideration that there are $2I$ different allowed transitions for a molecule in a given rotational state. The result of summing $R(\nu,J)$ for all J is as follows:

$$R(\nu)=2a^2\int_0^\infty R(\nu,J)J\exp(-a^2J^2)dJ. \tag{16}$$

If Eq. (15) is used in Eq. (16) with z determined by Eq. (2a) and (2c), Eq. (5) follows.

For the transition $\frac{1}{2}\leftrightarrow-\frac{1}{2}$ the second-order terms (Eq. (2b)) need be considered. This calculation is different in that z is a multi-valued function of $\bar{\nu}$. The calculation is of sufficient complexity to warrant the neglect of the term in $1/J$. For a given value of $\bar{\nu}$ there are in general two allowable values of $z(|z|\leqslant 1)$, z_+ and z_-. Equation (15) then becomes

$$R(\nu)=(K_1K_2/2I)\,|[z_-(\nu+\Delta\bar{\nu})-z_-(\nu-\Delta\bar{\nu})] -[z_+(\nu+\Delta\bar{\nu})-z_+(\nu-\Delta\bar{\nu})]|. \tag{17}$$

(Equations (15) and (17) may be used explicitly for all values of ν, if the convention be adopted that z, z_+, or z_- is to be taken as zero whenever it becomes imaginary, or to be taken as unity whenever it exceeds unity.) Substitution of $\nu=\nu_I+\frac{3}{4}x_0^2\nu_I-\Delta\bar{\nu}$ and $I=\frac{3}{2}$ in Eq. (17), together with z determined by Eq. (2b), yields for the intensity at the upper frequency minimum of the central minimum

$$R(\nu_I+\tfrac{3}{4}x_0^2\nu_I-\Delta\bar{\nu})=\tfrac{1}{3}K_1K_2(4\Delta\bar{\nu}/15x_0^2\nu_I)^{\frac{1}{2}}.$$

APPENDIX II. ENERGY LEVELS IN STRONG AND WEAK FIELDS

The Hamiltonian used to analyze the results of the experiments reported is:

$$\mathcal{H}=-\mu_N g_I\mathbf{I}\cdot\mathbf{H}+\frac{e^2qQ}{2I(2I-1)J(2J-1)}\{3(\mathbf{I}\cdot\mathbf{J})^2 +\tfrac{3}{2}(\mathbf{I}\cdot\mathbf{J})-I(I+1)J(J+1)\}-c\mathbf{I}\cdot\mathbf{J}. \tag{18}$$

Strong Field

The matrix elements of each term of the Hamiltonian in the m_I and m_J representation are most conveniently stated in reference 4. The calculation of the energy levels to the second order in e^2qQ and c, considering $-\mu_N g_I\mathbf{I}\cdot\mathbf{H}$ the unperturbed Hamiltonian, yields for J large and $I=\frac{3}{2}$:

$$W_{3/2}=-\tfrac{3}{2}\mu_N g_I H+\tfrac{1}{2}b(3z^2-1)-\tfrac{3}{2}cJ_z -\frac{[\sqrt{3}bz-c\frac{1}{2}\sqrt{3}J]^2(1-z^2)}{\mu_N g_I H}-\frac{\frac{3}{4}b^2(1-z^2)^2}{2\mu_N g_I H} \tag{19a}$$

$$W_{\frac{1}{2}}=-\tfrac{1}{2}\mu_N g_I H-\tfrac{1}{2}b(3z^2-1)-\tfrac{1}{2}cJ_z +\frac{[\sqrt{3}bz-c\frac{1}{2}\sqrt{3}J]^2(1-z^2)}{\mu_N g_I H}-\frac{c^2J^2(1-z^2)}{\mu_N g_I H}-\frac{\frac{3}{4}b^2(1-z^2)^2}{2\mu_N g_I H} \tag{19b}$$

$$W_{-\frac{1}{2}}=\tfrac{1}{2}\mu_N g_I H-\tfrac{1}{2}b(3z^2-1)+\tfrac{1}{2}cJ_z -\frac{[-\sqrt{3}bz-c\frac{1}{2}\sqrt{3}J]^2(1-z^2)}{\mu_N g_I H}+\frac{c^2J^2(1-z^2)}{\mu_N g_I H}+\frac{\frac{3}{4}b^2(1-z^2)^2}{2\mu_N g_I H} \tag{19c}$$

$$W_{-3/2}=\tfrac{3}{2}\mu_N g_I H+\tfrac{1}{2}b(3z^2-1)+\tfrac{3}{2}cJ_z +\frac{[-\sqrt{3}bz-c\frac{1}{2}\sqrt{3}J]^2(1-z^2)}{\mu_N g_I H}+\frac{\frac{3}{4}b^2(1-z^2)^2}{2\mu_N g_I H} \tag{19d}$$

with $b=e^2qQ/4$.

[14] G. C. Wick, Zeits. f. Physik **85**, 25 (1933).
[15] N. F. Ramsey, Phys. Rev. **58**, 226 (1940).

The energy differences are

$$W_{3/2}-W_{\frac{1}{2}}=-\mu_N g_I H-cJ_z+b(3z^2-1) -\frac{6b^2z^2(1-z^2)}{\mu_N g_I H}-\frac{1}{2}\frac{c^2J^2(1-z^2)}{\mu_N g_I H}+\frac{6bcJ_z(1-z^2)}{\mu_N g_I H} \quad (20a)$$

$$W_{\frac{1}{2}}-W_{-\frac{1}{2}}=-\mu_N g_I H-cJ_z +\frac{3}{4}\frac{b^2(1-z^2)(9z^2-1)}{\mu_N g_I H}-\frac{1}{2}\frac{c^2J^2(1-z^2)}{\mu_N g_I H}, \quad (20b)$$

$$W_{-\frac{1}{2}}-W_{-3/2}=-\mu_N g_I H-cJ_z-b(3z^2-1) -\frac{6b^2z^2(1-z^2)}{\mu_N g_I H}-\frac{1}{2}\frac{c^2J^2(1-z^2)}{\mu_N g_I H}-\frac{6bcJ_z(1-z^2)}{\mu_N g_I H}. \quad (20c)$$

Equation (6) of the text follows by dividing through by $-\mu_N g_I H$.

Zero Field

The Hamiltonian is diagonal in the $\mathbf{F}=\mathbf{I}+\mathbf{J}$ and m_F representation. The energy differences are, for large J

$$W_{3/2}-W_{\frac{1}{2}}=-\tfrac{1}{2}e^2q'Q-cJ, \quad (21a)$$

$$W_{\frac{1}{2}}-W_{-\frac{1}{2}}=(3e^2q'Q/4J)-cJ, \quad (21b)$$

$$W_{-\frac{1}{2}}-W_{-3/2}=\tfrac{1}{2}e^2q'Q-cJ. \quad (21c)$$

Neglecting the transition $\frac{1}{2}\leftrightarrow-\frac{1}{2}$ the spectrum will be situated about the frequency $\nu_I^0=e^2q'Q/2h$, and the transition frequency is given by

$$\bar{\nu}=e^2q'Q/2h\pm cJ/h. \quad (22)$$

APPENDIX III. EFFECT OF THE $c\mathbf{I}\cdot\mathbf{J}$ TERM ON THE LINE SHAPE

Zero Field

Assuming $e^2q'Q\gg(cJ)_{\text{Av}}$, the line shape can be calculated in a straightforward fashion. $d\bar{\nu}/dJ=c/h$ and $dN/dJ=2a^2J\exp(-a^2J^2)$, and, therefore,

$$dN/d\bar{\nu}=\tfrac{2}{3}(ah/c)^2|\bar{\nu}-\nu_I^0|\exp[-(ha/c)^2(\bar{\nu}-\nu_I^0)^2]. \quad (23)$$

The factor $\frac{1}{3}$ is inserted to normalize the total transitions to unity. If there is no quadrupole interaction $\nu_I^0=0$. Repeating the calculation for $e^2qQ=0$, the line shape is given by

$$dN/d\bar{\nu}=2(ah/c)^2\bar{\nu}\exp[-(ha/c)^2\bar{\nu}^2]. \quad (24)$$

This is Eq. (13) of the text.

Strong Field

In the absence of a quadrupole moment, $(b=0)$, the strong-field frequencies are given, from Eq. (20), by

$$\bar{\nu}=\nu_I+cm_J/h. \quad (25)$$

Again, $d\bar{\nu}/dm_J=c/h$, but

$$dN/dm_J=a^2\int_{m_J}^{\infty}\exp(-a^2J^2)dJ$$

for $m_J\gtrsim 0$ or,

$$dN/d\bar{\nu}=(ha/c)\int_{am_J}^{\infty}\exp(-v^2)dv, \quad m_J\gtrsim 0, \quad (26)$$

and therefore

$$dN/d\bar{\nu}=(ha\sqrt{\pi}/2c)\{1-\text{erf}[(ha/c)|\bar{\nu}-\nu_I|]\} \text{ all } m_J. \quad (27)$$